JACC: BASIC TO TRANSLATIONAL SCIENCE VOL. 4, NO. 2, 2019

PRECLINICAL RESEARCH

Cardiac Nuclear High-Mobility Group Box 1 Ameliorates Pathological Cardiac Hypertrophy by Inhibiting DNA Damage Response

Tetsuya Takahashi, MD,[a] Tetsuro Shishido, MD, PHD,[a] Daisuke Kinoshita, MD, PHD,[a] Ken Watanabe, MD,[a] Taku Toshima, MD,[a] Takayuki Sugai, MD,[a] Taro Narumi, MD, PHD,[a] Yoichiro Otaki, MD, PHD,[a] Harutoshi Tamura, MD, PHD,[a] Satoshi Nishiyama, MD, PHD,[a] Takanori Arimoto, MD, PHD,[a] Hiroki Takahashi, MD, PHD,[a] Takuya Miyamoto, MD, PHD,[a] Tetsu Watanabe, MD, PHD,[a] Chang-Hoon Woo, DVM, PHD,[b] Jun-ichi Abe, MD, PHD,[c] Yasuchika Takeishi, MD, PHD,[d] Isao Kubota, MD, PHD,[a] Masafumi Watanabe, MD, PHD[a]

VISUAL ABSTRACT

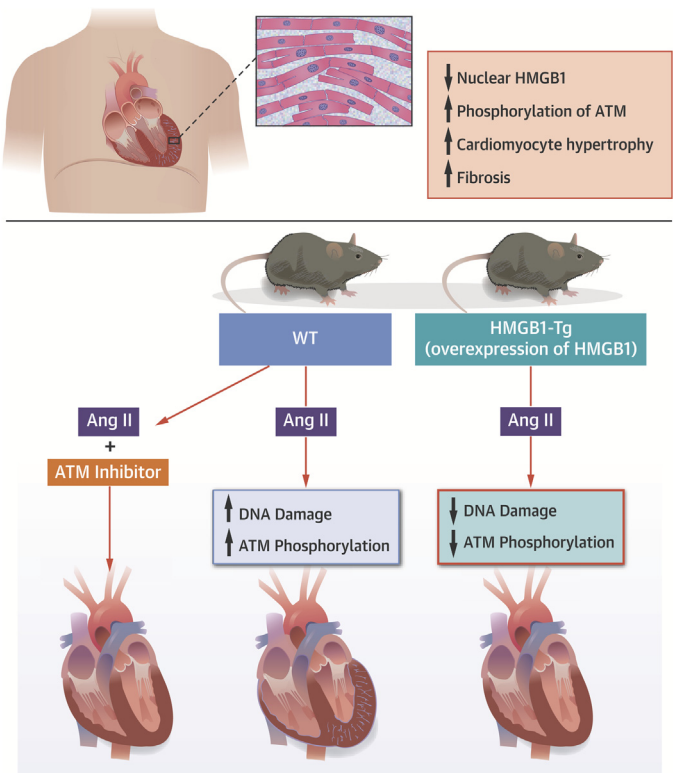

Takahashi, T. et al. J Am Coll Cardiol Basic Trans Science. 2019;4(2):234–47.

HIGHLIGHTS

- **HMGB1 is a DNA-binding protein associated with nuclear homeostasis and DNA repair.**
- **Decreased nuclear HMGB1 expression is observed in human failing hearts, which is associated with cardiomyocyte hypertrophy and fibrosis.**
- **Cardiac nuclear HMGB1 overexpression ameliorates Ang II–induced pathological cardiac remodeling by inhibiting cardiomyocyte DNA damage and following ataxia telangiectasia mutated activation in mice.**
- **Ataxia telangiectasia mutated inhibitor treatment provided a cardioprotective effect on Ang II–induced cardiac remodeling in mice.**

From the [a]Department of Cardiology, Pulmonology, and Nephrology, Yamagata University School of Medicine, Yamagata, Japan; [b]Department of Pharmacology, College of Medicine, Yeungnam University, Daegu, Republic of Korea; [c]Department of Cardiology - Research, Division of Internal Medicine, University of Texas MD Anderson Cancer Center, Houston, Texas; and the [d]Department of Cardiology and Hematology, Fukushima Medical University, Fukushima, Japan. This study was supported in part by a Grant-in-Aid

ISSN 2452-302X https://doi.org/10.1016/j.jacbts.2018.11.011

SUMMARY

High-mobility group box 1 (HMGB1) is a deoxyribonucleic acid (DNA)–binding protein associated with DNA repair. Decreased nuclear HMGB1 expression and increased DNA damage response (DDR) were observed in human failing hearts. DNA damage and DDR as well as cardiac remodeling were suppressed in cardiac-specific HMGB1 overexpression transgenic mice after angiotensin II stimulation as compared with wild-type mice. In vitro, inhibition of HMGB1 increased phosphorylation of extracellular signal-related kinase 1/2 and nuclear factor kappa B, which was rescued by DDR inhibitor treatment. DDR inhibitor treatment provided a cardioprotective effect on angiotensin II–induced cardiac remodeling in mice. (J Am Coll Cardiol Basic Trans Science 2019;4:234–47)

Heart failure is a common disease and has been increasing worldwide (1,2). Despite advances in the treatment of heart failure, patients with heart failure are faced with a poor prognosis (3). Cardiac remodeling, characterized by cardiac hypertrophy and fibrosis, is closely associated with the development of heart failure and death (4,5). It is well known that neurohumoral activation such as angiotensin II (Ang II) is one of the major risk factors for pathological cardiac remodeling and subsequent heart failure (6). However, treatment that is able to sufficiently suppress pathological cardiac remodeling has not been established yet.

SEE PAGE 248

High-mobility group box 1 (HMGB1) is an abundant chromatin-associated nuclear nonhistone binding protein, which has various functions in maintaining cellular homeostasis (7,8). HMGB1 translocates to extracellular from intracellular under various stress situations, and acts as a damage-associated molecular pattern (DAMP) that triggers several inflammatory responses (9,10). Extracellular HMGB1 was reported to cause cardiac hypertrophy and promote myocardial ischemia or reperfusion injury and inflammation (11–13). In contrast, intracellular HMGB1 plays roles in maintaining nucleosome structure, regulating gene transcription, replication, and DNA repair (7,8). Recently, it was reported that intracellular HMGB1 has a more important role in cell fate than extracellular HMGB1 during some inflammatory diseases since ablation of nuclear HMGB1 worsens disease condition (14–16). We previously reported that cardiac nuclear HMGB1 prevents cardiomyocyte deoxyribonucleic acid (DNA) damage in a pressure overload heart failure mouse model (17). However, the molecular mechanism underlying the antihypertrophic effect of cardiac nuclear HMGB1 has not been fully elucidated.

Various types of stress cause cellular DNA damage, and the DNA damage response (DDR) is induced immediately after DNA damage to repair it (18). Activation of the DDR occurs after excessive DNA damage and is reported to be observed in end-stage failing human hearts (19). Moreover, previous studies have revealed that DDR activation plays a crucial role in development of cardiac remodeling after myocardial infarction and cardiac hypertrophy (20,21).

We hypothesized that cardiac nuclear HMGB1 suppresses pathological cardiac remodeling through inhibition of DDR activation.

METHODS

A detailed description of all experimental procedures is provided in the Supplemental Appendix.

ABBREVIATIONS AND ACRONYMS

Ang II = angiotensin II
ANP = atrial natriuretic peptide
ATM = ataxia telangiectasia mutated
BNP = brain natriuretic peptide
CVF = collagen volume fraction
DAMP = damage-associated molecular pattern
DDR = deoxyribonucleic acid damage response
DNA = deoxyribonucleic acid
E/A ratio = ratio of early to atrial wave
ERK1/2 = extracellular signal-related kinase 1/2
HMGB1 = high-mobility group box 1
HMGB1-Tg = high-mobility group box 1 transgenic
HW/TL = heart weight to tibial length
IVSd = interventricular septum diameter
LVDd = left ventricular diastolic dimension
LVDs = left ventricular systolic dimension
MyD = cardiomyocyte diameter
NF-κB = nuclear factor kappa B
NRCM = neonatal rat cardiomyocyte
p-ATM = phosphorylation of ataxia telangiectasia mutated
PWd = posterior wall diameter
WT = wild-type

from the 21st Century of Excellence (COE) and Global COE program of the Japan Society for the Promotion of Science (No. F03), and a grant-in-aid for Scientific Research (18K08025, 18K08059, and 16K09490) from the Ministry of Education, Culture, Sports, Science, and Technology, Japan. The authors have reported that they have no relationships relevant to the contents of this paper to disclose.

All authors attest they are in compliance with human studies committees and animal welfare regulations of the authors' institutions and Food and Drug Administration guidelines, including patient consent where appropriate. For more information, visit the *JACC: Basic to Translational Science* author instructions page.

Manuscript received July 9, 2018; revised manuscript received October 19, 2018, accepted November 19, 2018.

HUMAN STUDIES. This study included 27 patients with heart failure and 5 control patients who were assessed to rule out cardiomyopathy and had normal cardiac function. Written informed consent was obtained from all patients before entry into the study. The protocol was performed in accordance to the Helsinki Declaration and was approved by the human investigations committee of our institution. Biopsy samples were immediately washed in phosphate-buffered saline before being snap-frozen in liquid nitrogen for immunofluorescent co-staining and biochemical measurements. Immunofluorescence was performed to evaluated the expressions of cardiac nuclear HMGB1, phosphorylation of ataxia telangiectasia mutated (p-ATM), and γ-H2AX in failing (n = 5) and normal human hearts (n = 5). The heart sections were stained with hematoxylin and eosin to assess cardiomyocyte diameter (MyD). The degree of collagen volume fraction (CVF) was assessed by Masson's trichrome staining as previously described (22). Blood samples were obtained to measure brain natriuretic peptide (BNP) levels. Correlations between nuclear HMGB1 levels and MyD, CVF, and serum BNP levels were assessed (n = 32).

ANIMAL MODELS. Cardiac hypertrophy was induced in 10- to 12-week-old mice with cardiac-specific overexpression of HMGB1 (HMGB1-Tg) and their wild-type (WT) littermates by chronic infusion of Ang II (1.5 mg/kg/day) or saline as previously described (23). For ATM inhibitor experiments, KU55933 (5 mg/kg) or vehicle was injected intraperitoneally to HMGB1-Tg mice at 2, 5, 8, and 11 days after Ang II infusion. After 2 weeks, blood pressure, cardiac function, and dimension were measured. The hearts were removed for examination of histological changes and biochemical analysis of various protein expression levels.

ECHOCARDIOGRAPHY DETERMINATION. Transthoracic echocardiography was performed before and after Ang II infusion under anesthesia as previously described (24). Left ventricular diastolic dimension (LVDd), left ventricular systolic dimension (LVDs), interventricular septum diameter (IVSd), posterior wall diameter (PWd), left ventricular fractional shortening (FS), and the transmitral Doppler velocity ratio of early to atrial wave (E/A ratio) were measured (n = 10 in WT saline group; n = 10 in WT Ang II group; n = 6 in HMGB1-Tg saline group; n = 6 in HMGB1-Tg Ang II group). As for ATM inhibitor experiments, the same parameters were also measured (n = 9 in WT vehicle group; n = 10 in WT Ang II + vehicle group; n = 6 in HMGB1-Tg Ang II + vehicle group; n = 6 in WT Ang II + KU55933 group; n = 6 in HMGB1-Tg Ang II + KU55933 group).

CELL CULTURE AND TREATMENT. Primary culture of neonatal rat cardiomyocytes (NRCMs) was performed as previously described (25,26). HMGB1 small interfering ribonucleic acid (siHMGB1), pcDNA-HMGB1 were transfected into NRCMs by using Lipofectamine 3000 Reagent (Invitrogen, Carlsbad, California) according to the manufacturer's instructions. After serum starvation for 24 h, cardiomyocytes were stimulated with 1-μM Ang II for 24 h to induce cardiac hypertrophy, and samples were collected to perform each experiment. For ATM inhibitor experiments, cardiomyocytes were pretreated with KU55933 (10 μM) for 1 h before Ang II stimulation.

STATISTICAL ANALYSIS. Data are presented as the mean ± SE. Statistical significance was evaluated using unpaired Student *t* test with Welch correction for comparing 2 groups. Comparing ≥3 groups were done using 1-way analysis of variance. Post hoc pairwise comparisons were done using the Tukey-Kramer method. Correlation between 2 variables was examined by using Pearson's product moment correlation coefficient. Because CVF and BNP were not normally distributed, we used $\log_{10}$ CVF and $\log_{10}$ BNP values in the Pearson correlation analysis. A value of $p < 0.05$ was considered statistically significant. All statistical analyses were performed using a standard statistical program package (JMP version 11, SAS Institute Inc., Cary, North Carolina).

RESULTS

EXPRESSION OF HMGB1 IN FAILING HUMAN HEARTS. We investigated the expression of nuclear HMGB1, DNA damage, and DDR in failing and normal human hearts. Immunofluorescence demonstrated that nuclear HMGB1 expression was significantly decreased and p-ATM expression was significantly increased in failing hearts compared with that of normal hearts (**Figures 1A to 1C**). γ-H2AX is known as an early and sensitive marker of DNA damage (27). The expression of γ-H2AX was also significantly increased in failing hearts compared with those of normal hearts (Supplemental Figures 1A to 1C). We evaluated the relationship among cardiomyocyte diameter, collagen volume fraction, serum BNP levels, and nuclear HMGB1 expression levels. A significant negative correlation was observed between nuclear HMGB1 levels and MyD, CVF, and BNP levels (**Figures 1D to 1F**).

THE PROTECTIVE EFFECT OF NUCLEAR HMGB1 ON PATHOLOGICAL CARDIAC REMODELING INDUCED BY ANG II. To investigate the potential role of nuclear HMGB1 in pathological cardiac remodeling, we subjected WT and HMGB1-Tg mice to Ang II

FIGURE 1 **Nuclear HMGB1 and p-ATM Expression in Failing Human Heart**

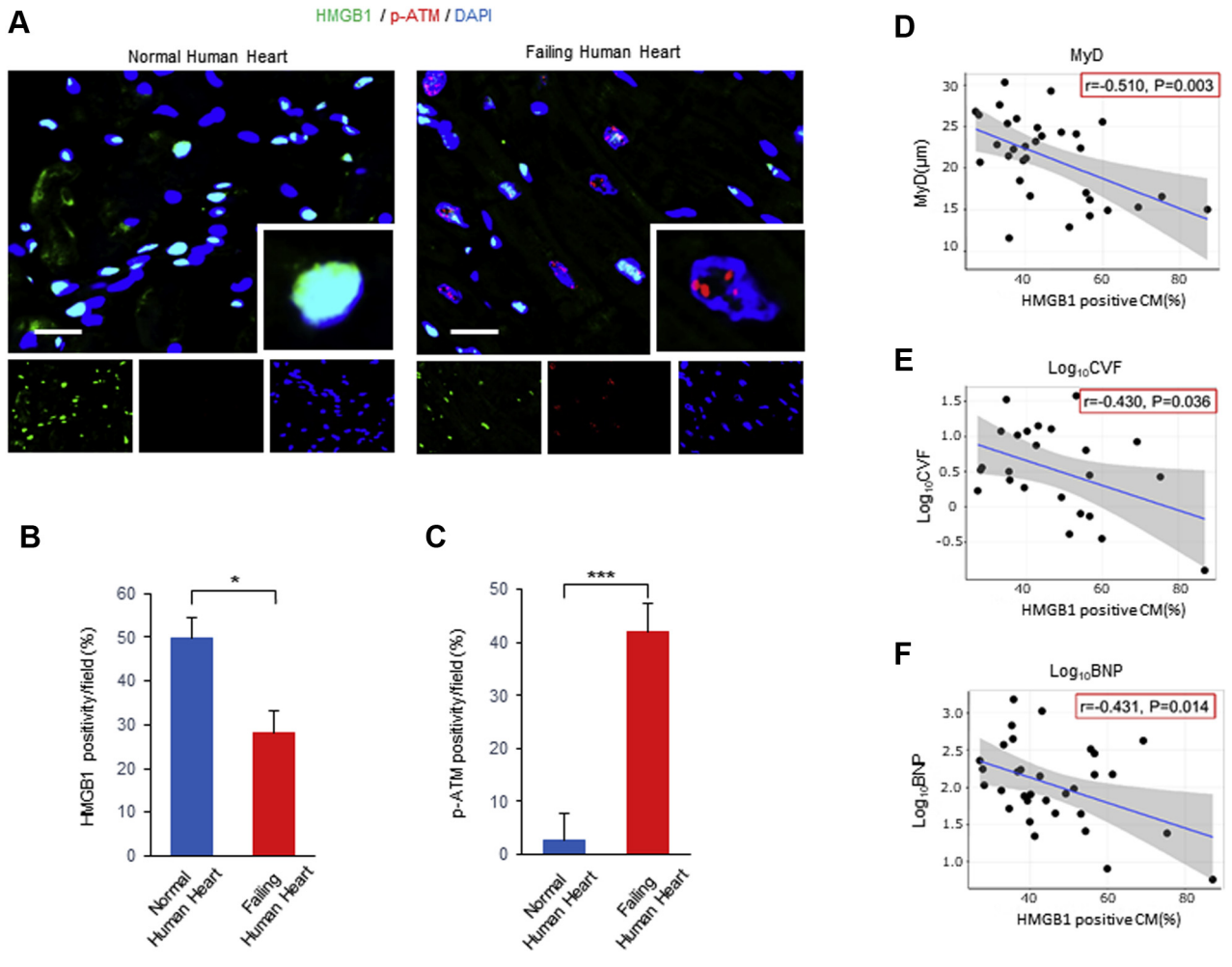

(A to C) Representative images and analysis of immunostaining of high-mobility group box 1 (HMGB1) **(green)**, phosphorylation of ataxia telangiectasia mutated (p-ATM) **(red)**, and DAPI **(blue)** in normal human hearts and failing human hearts. The number of HMGB1- and p-ATM-positive cardiomyocytes (CMs) per field was counted. Scale bars = 20 μm. Results are presented as the mean ± SE. (n = 5 per group). *$p < 0.05$; ***$p < 0.001$. **(D to F)** Negative correlation between nuclear HMGB1-positive CM and cardiomyocyte diameter (MyD), collagen volume fraction (CVF), or serum brain natriuretic peptide (BNP) levels (n = 32).

infusion for 2 weeks. After Ang II infusion, WT mice exhibited significant increases in the IVSd and PWd, whereas HMGB1-Tg mice showed a reduction in hypertrophic changes. There were no significant differences in the LVDd, LVDs, and FS between WT and HMGB1-Tg mice. The E/A ratio was significantly decreased in WT mice after Ang II infusion whereas the E/A ratio of HMGB1-Tg mice was attenuated (**Table 1**, Supplemental Figure 2).

There was no significant difference in blood pressure after Ang II infusion between WT and HMGB1-Tg mice (**Table 2**). Histological analysis with hematoxylin and eosin staining revealed that the cardiomyocyte hypertrophy induced by Ang II was significantly attenuated in the HMGB1-Tg mice compared with that of the WT mice (**Figures 2A and 2B**). Ang II infusion also resulted in an increase in the heart weight to tibial length (HW/TL) ratio in WT mice, whereas the increase in the HW/TL ratio was suppressed in HMGB1-Tg mice (**Figure 2C**). Masson's trichrome staining also demonstrated that HMGB1-Tg mice showed less fibrosis after Ang II infusion compared with that of WT mice (**Figures 2D and 2E**). These results suggest that cardiac nuclear HMGB1 protects against Ang II-induced pathological cardiac remodeling.

TABLE 1 Echocardiographic Data of WT and HMGB1-Tg Mice Following Saline or Ang II Infusion

	WT Saline (n = 10)	WT Ang II (n = 10)	HMGB1-Tg Saline (n = 6)	HMGB1-Tg Ang II (n = 6)
LVDd, mm	3.43 ± 0.11	3.35 ± 0.11	3.43 ± 0.11	3.47 ± 0.11
LVDs, mm	1.82 ± 0.08	1.86 ± 0.08	1.86 ± 0.08	1.89 ± 0.08
IVSd, mm	0.61 ± 0.03	1.03 ± 0.03*	0.66 ± 0.03	0.72 ± 0.03†
PWd, mm	0.71 ± 0.03	1.02 ± 0.03*	0.71 ± 0.03	0.77 ± 0.03†
FS, %	47.0 ± 1.4	43.7 ± 1.4	45.8 ± 1.4	45.8 ± 1.4
E/A ratio	1.85 ± 0.05	1.11 ± 0.05*	1.80 ± 0.06	1.47 ± 0.06†‡

Values are mean ± SE. *p < 0.001 versus WT saline mice. †p < 0.001 versus WT Ang II mice. ‡p < 0.01 versus HMGB1-Tg saline mice.

Ang II = angiotensin II; E/A ratio = ratio of early to atrial wave; FS = fractional shortening; MGB1-Tg = cardiac-specific high-mobility group box 1 overexpression transgenic mice; IVSd = interventricular septum diameter; LVDd = left ventricular diastolic dimension; LVDs = left ventricular systolic dimension; PWd = posterior wall diameter; HWT = wild-type mice.

THE PROTECTIVE EFFECT OF CARDIAC NUCLEAR HMGB1 ON DNA DAMAGE AND DDR IN VIVO. We next examined whether cardiac nuclear HMGB1 overexpression prevents DNA damage and DDR in vivo. Immunofluorescence revealed that nuclear γ-H2AX-positive cardiomyocytes was increased in WT mice, whereas HMGB1-Tg mice showed attenuated γ-H2AX expression after Ang II infusion (**Figures 3A and 3B**). Western blot analysis also showed that decreased γ-H2AX expression was observed in HMGB1-Tg mice compared with that of WT mice after Ang II infusion (**Figures 3C and 3D**). Ang II infusion resulted in a significant increase in the p-ATM positive cardiomyocytes in WT mice, whereas HMGB1-Tg mice showed less p-ATM positive cardiomyocytes (**Figures 3E and 3F**). Western blot analysis showed that p-ATM was significantly lower in HMGB1-Tg mice compared with that of WT mice after Ang II infusion (**Figures 3G and 3H**). These data suggest that cardiac nuclear HMGB1 protects against Ang II-induced DNA damage and DDR.

TABLE 2 Hemodynamic Data of WT and HMGB1-Tg Mice Following Saline or Ang II Infusion

	WT Saline (n = 14)	WT Ang II (n = 10)	HMGB1-Tg Saline (n = 15)	HMGB1-Tg Ang II (n = 10)
BW, g	25.7 ± 0.6	27.1 ± 0.6	26.3 ± 0.6	26.8 ± 0.6
Hemodynamic parameter				
HR, beats/min	608 ± 17	612 ± 20	586 ± 16	615 ± 20
SBP, mm Hg	92 ± 3.3	142 ± 3.9*	95 ± 3.2	138 ± 3.9†
DBP, mm Hg	36 ± 5.7	95 ± 6.8‡	32 ± 5.5	69 ± 6.7†
MBP, mm Hg	55 ± 4.6	111 ± 5.5*	51 ± 4.5	92 ± 5.5†

Values are mean ± SE. *p < 0.001 versus WT saline mice. †p < 0.001 versus HMGB1-Tg saline mice. ‡p < 0.01versus WT saline mice.

BW = body weight; DBP = diastolic blood pressure; HR = heart rate; MBP = mean blood pressure; SBP = systolic blood pressure; other abbreviations as in Table 1.

IMPACT OF NUCLEAR HMGB1 ON HYPERTROPHIC RESPONSE INDUCED BY ANG II IN VITRO. We examined the effect of HMGB1 on the hypertrophic response in cultured NRCMs. Immunostaining of NRCMs for α-actinin indicated that HMGB1 overexpression significantly attenuated the increase in cardiomyocyte hypertrophy induced by Ang II (Supplemental Figures 3A and 3B). In contrast, HMGB1 knockdown promoted the hypertrophic growth of cardiomyocytes in response to Ang II (Supplemental Figures 3C and 3D). These data indicated that cardiac nuclear HMGB1 prevents cardiomyocyte hypertrophy in response to Ang II stimulation.

THE PROTECTIVE EFFECT OF CARDIAC NUCLEAR HMGB1 ON DNA DAMAGE AND DDR IN VITRO. We determined whether HMGB1 regulates DNA damage and the DDR in NRCMs after Ang II stimulation. Bimodal upregulation of p-ATM and γ-H2AX were observed 2 and 24 h after Ang II stimulation in NRCMs. In contrast, nuclear HMGB1 expression was decreased 1 and 24 h after Ang II stimulation in NRCMs (Supplemental Figure 4). HMGB1 overexpression resulted in a significant decrease in the number of nuclear γ-H2AX foci (**Figures 4A and 4B**). Western blot analysis showed that γ-H2AX expression was attenuated in HMGB1 overexpression NRCMs (**Figures 4C and 4D**). HMGB1 overexpression also decreased the number of nuclear p-ATM foci induced by Ang II stimulation (**Figures 4E and 4F**). Western blot analysis demonstrated that p-ATM was also attenuated in HMGB1 overexpression NRCMs (**Figures 4G and 4H**).

In contrast, HMGB1 knockdown significantly increased the number of nuclear γ-H2AX foci in NRCMs after Ang II stimulation (**Figures 5A and 5B**). Western blot analysis also revealed that γ-H2AX expression was further enhanced in HMGB1 knockdown NRCMs after Ang II stimulation (**Figures 5C and 5D**). HMGB1 knockdown significantly increased the number of nuclear p-ATM foci in NRCMs (**Figures 5E and 5F**), and p-ATM expression was enhanced in HMGB1 knockdown NRCMs after Ang II stimulation (**Figures 5G and 5H**). These data suggested that nuclear HMGB1 regulates Ang II-induced DNA damage and the DDR in vitro.

THE IMPACT OF HMGB1 AND ATM ON ANG II–INDUCED CARDIAC HYPERTROPHIC RESPONSE. To investigate further mechanisms by which HMGB1 and DDR are involved in Ang II-induced hypertrophic response, the association between HMGB1 and ATM was examined by immunoprecipitation experiments. Immunoprecipitation revealed a potential interaction between HMGB1 and ATM in NRCMs (Supplemental Figures 5A and 5B). In addition, Ang II

FIGURE 2 **Cardiac Nuclear HMGB1 Protects Mice Against Ang II–Induced Cardiac Remodeling**

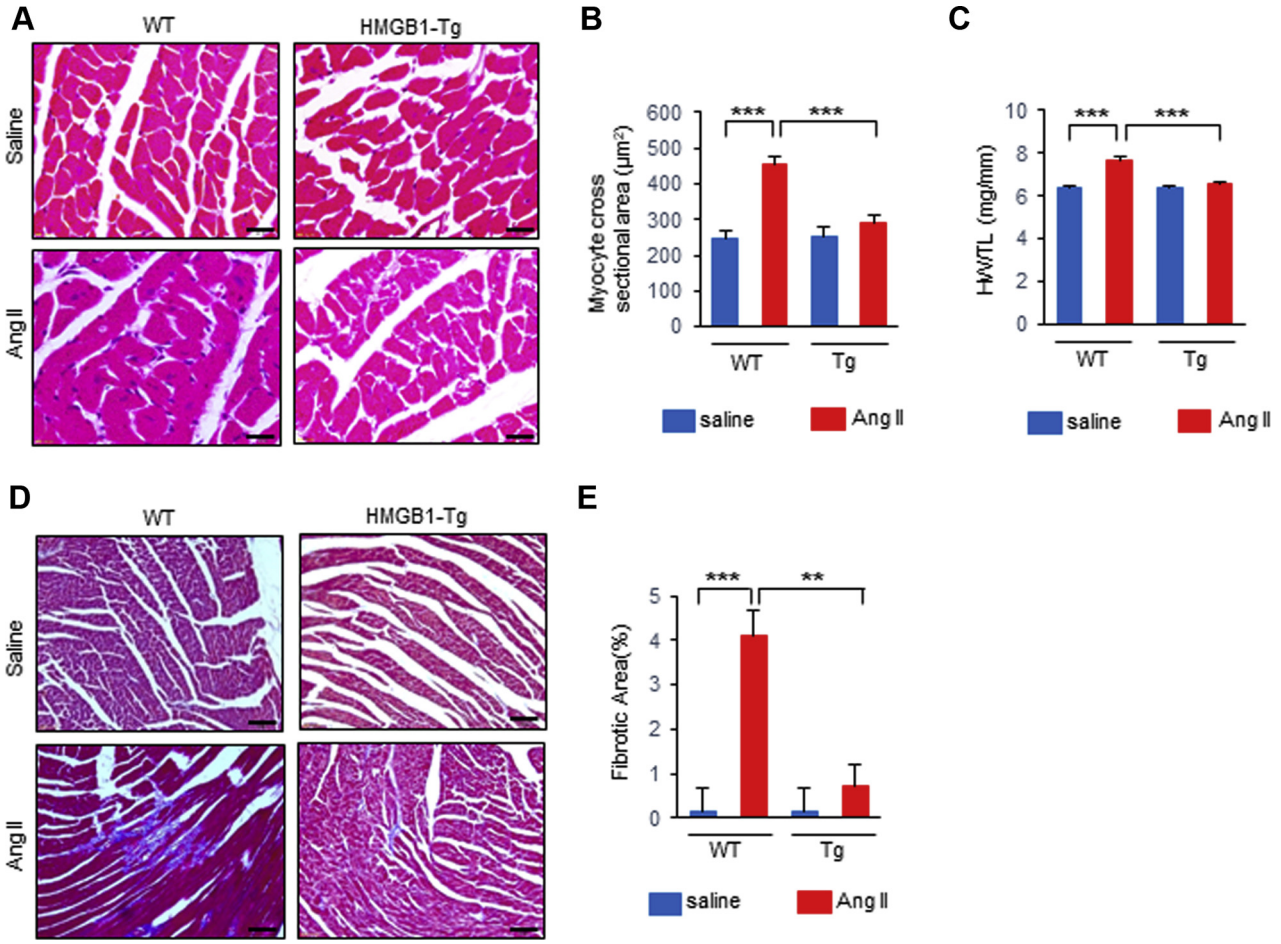

(A, B) Representative images and analysis of CM cross-sectional area from hematoxylin and eosin (H&E)–stained left ventricular sections in wild-type (WT) and HMGB1 transgenic (HMGB1-Tg) mice following saline or angiotensin II (Ang II) infusion. Scale bars = 20 μm. (n = 6 per group). **(C)** The ratio of heart weight to tibial length (HW/TL) in WT and HMGB1-Tg mice following saline or Ang II infusion (n = 10 per group). **(D, E)** Representative images and analysis of cardiac fibrosis area by Masson's trichrome staining in left ventricular sections in WT and HMGB1-Tg mice following saline or Ang II infusion. Scale bars = 50 μm. n = 5 in WT saline group; n = 4 in WT Ang II group; n = 5 in HMGB1-Tg saline group; n = 5 in HMGB1-Tg Ang II group. Results are presented as the mean ± SE. **$p < 0.01$; ***$p < 0.001$. Abbreviations as in Figure 1.

stimulation decreased the interaction between HMGB1 and ATM (Supplemental Figure 5C).

Next, we analyzed the effect of HMGB1 on activation of the hypertrophic signaling pathway. HMGB1 overexpression significantly attenuated the phosphorylation of ERK1/2 and nuclear factor kappa B (NF-κB) induced by Ang II in NRCMs (**Figures 6A and 6B**). HMGB1 knockdown exhibited enhanced Ang II mediated activation of the ERK1/2 and NF-κB pathway (**Figures 6C and 6D**). We examined the effect of ATM on hypertrophic signaling kinases in NRCMs using a specific ATM inhibitor KU55933. Ang II–induced phosphorylation of ERK1/2 and NF-κB was reduced by treatment with an ATM inhibitor in NRCMs (Supplemental Figures 6A and 6B). Furthermore, the enhanced phosphorylation of ERK1/2 and NF-κB by Ang II stimulation in HMGB1 knockdown NRCMs was suppressed by treatment with an ATM inhibitor (**Figure 6E**). We also evaluated the impact of nuclear HMGB1 and ATM on fetal cardiac gene expression. Atrial natriuretic peptide (ANP) and BNP promoter activities were increased by Ang II stimulation in vitro (Supplemental Figures 7A and 7B). HMGB1 knockdown exhibited enhanced ANP and BNP promoter activities induced by Ang II, which was abolished after pretreatment with ATM inhibitor (**Figures 6F and 6G**).

FIGURE 3 Cardiac Nuclear HMGB1 Prevents Ang II–Induced DNA Damage and the DDR in Mice

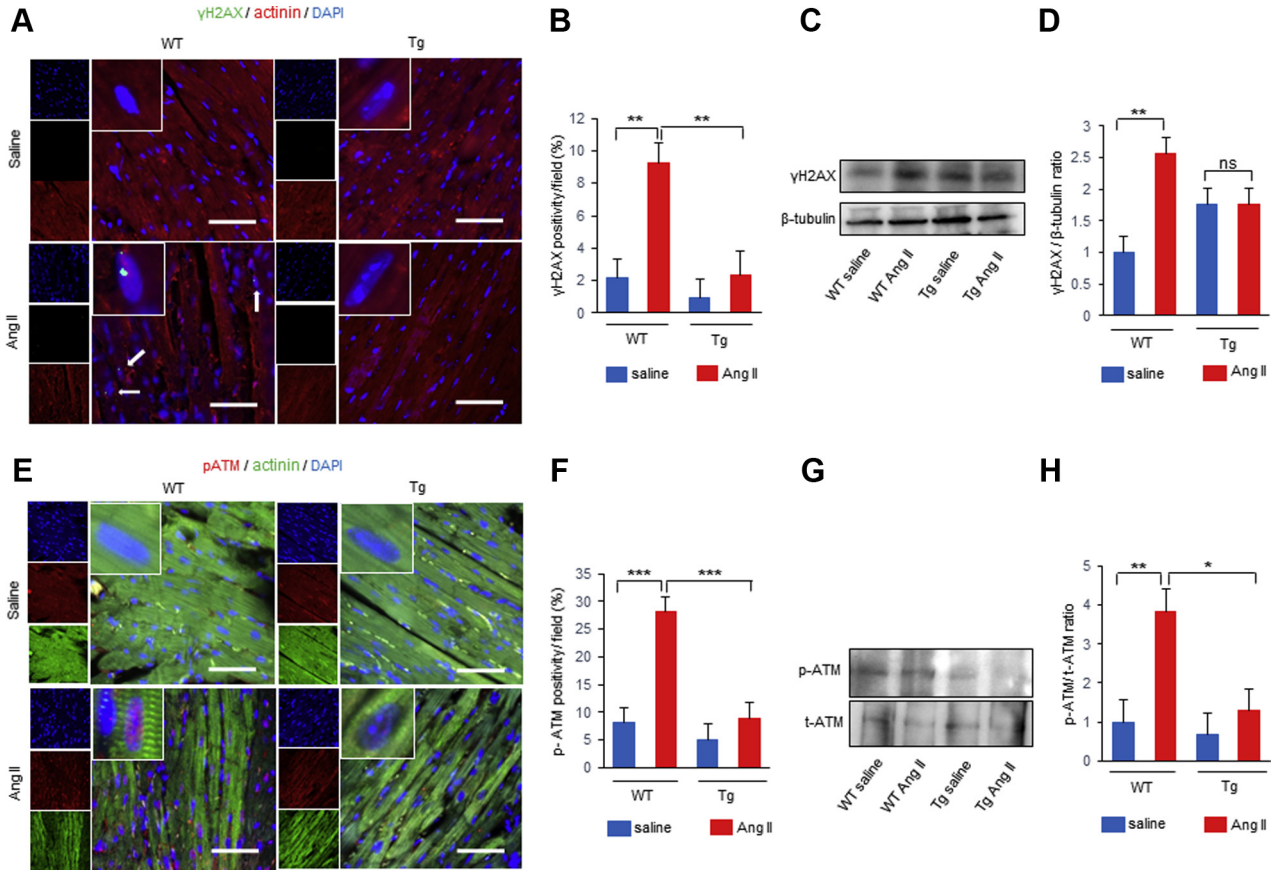

(A, B) Representative images and analysis of immunostaining of γ-H2AX **(green)**, α-actinin **(red)**, and DAPI **(blue)** in saline- or Ang II–treated WT and HMGB1-Tg mice. The number of γ-H2AX–positive CMs per field was counted. Scale bars = 50 μm. n = 6 in WT saline group; n = 6 in WT Ang II group; n = 6 in HMGB1-Tg saline group; n = 4 in HMGB1-Tg Ang II group. **(C, D)** Representative images and analysis of Western blots of γ-H2AX and β-tubulin from hearts of WT and HMGB1-Tg mice following saline or Ang II infusion (n = 5 per group). **(E, F)** Representative images and analysis of immunostaining of p-ATM **(red)**, α-actinin **(green)**, and DAPI **(blue)** in saline- or Ang II–treated WT and HMGB1-Tg mice. The number of p-ATM–positive CMs per field was counted. Scale bars = 50 μm. n = 6 in WT saline group; n = 7 in WT Ang II group; n = 5 in HMGB1-Tg saline group; n = 6 in HMGB1-Tg Ang II group. **(G, H)** Representative images and analysis of Western blots of p-ATM and total ATM from hearts of WT and HMGB1-Tg mice following saline or Ang II infusion (n = 6 per group). Results are presented as the mean ± SE. *$p < 0.05$; **$p < 0.01$; ***$p < 0.001$. DDR = deoxyribonucleic acid damage response; DNA = deoxyribonucleic acid; Other abbreviations as in Figures 1 and 2.

These results suggest that HMGB1 regulates Ang II–induced cardiac hypertrophy through inhibiting ATM activity.

THE CARDIOPROTECTIVE EFFECT OF PHARMACOLOGICAL ATM INHIBITION FOR ANG II–INDUCED PATHOLOGICAL CARDIAC REMODELING. To evaluate the therapeutic potential of ATM inhibitor, we treated WT and HMGB1-Tg mice with either ATM inhibitor or vehicle after Ang II infusion for 2 weeks (Figure 7A). Pharmacological ATM inhibition demonstrated cardioprotective effect in WT mice and also provided synergic cardioprotective effect in HMGB1-Tg mice for Ang II–induced pathological cardiac remodeling. WT and HMGB1 mice treated with the ATM inhibitor exhibited significant decrease in the IVSd and PWd compared with that of WT and HMGB1-Tg mice treated with vehicle after Ang II infusion. Pharmacological ATM inhibition did not alter the LVDd, whereas the FS was slightly improved in WT mice with ATM inhibitor. The E/A ratio was significantly improved when WT and HMGB1-Tg mice were treated with the ATM inhibitor after Ang II infusion compared with that of WT and HMGB1-Tg mice treated with vehicle after Ang II infusion (Table 3, Supplemental

FIGURE 4 Effect of HMGB1 Overexpression on DNA Damage and DDR After Ang II Stimulation

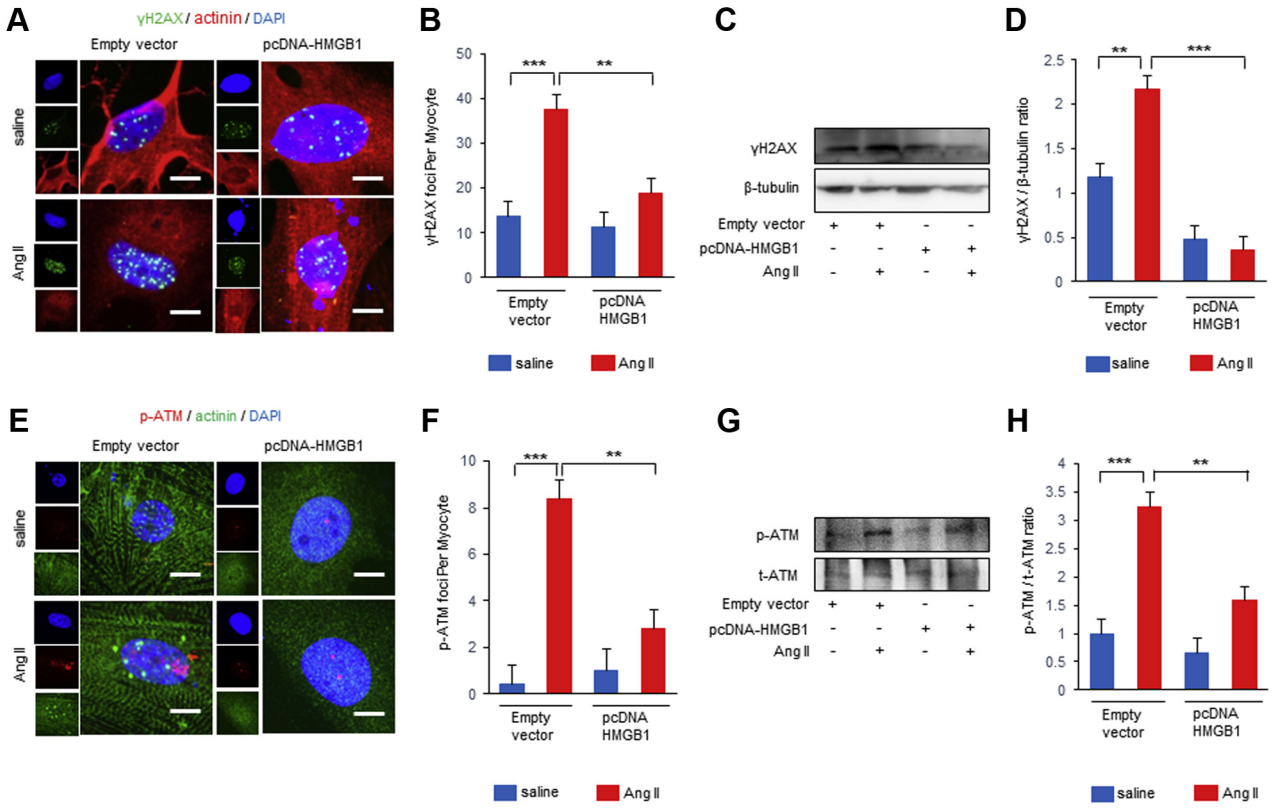

(A, B) Representative images and analysis of immunostaining of nuclear foci of γ-H2AX **(green)**, α-actinin **(red)**, and DAPI **(blue)** of neonatal rat CMs (NRCMs) transfected with pcDNA-HMGB1 or control vector and then treated with saline or Ang II for 24 h. The foci number of γ-H2AX per NRCM was counted. Scale bars = 20 μm. n = 6 per group. **(C, D)** Representative images and analysis of Western blots of γ-H2AX. NRCMs transfected with pcDNA-HMGB1 or control saline and then treated with vehicle or Ang II for 24 h (n = 5 per group). **(E, F)** Representative images and analysis of immunostaining of nuclear foci of p-ATM **(red)**, α-actinin **(green)**, and DAPI **(blue)** of NRCMs transfected with pcDNA-HMGB1 or control vector and then treated with saline or Ang II for 24 h. The foci number of p-ATM per NRCM was counted. Scale bars = 20 μm. n = 5 in control vector saline group; n = 5 in control vector Ang II group; n = 4 in pcDNA-HMGB1 saline group; n = 5 in pcDNA-HMGB1 Ang II group. **(G, H)** Representative images and analysis of Western blots of p-ATM and total ATM. NRCMs transfected with pcDNA-HMGB1 or control vector and then treated with saline or Ang II for 24 h (n = 4 per group). **p < 0.01; ***p < 0.001. Abbreviations as in Figures 1–3.

Figure 8). WT and HMGB1-Tg mice treated with the ATM inhibitor showed a lower HW/TL ratio than WT and HMGB1-Tg mice treated with vehicle after Ang II infusion (Figure 7B). ATM inhibitor treatment provided no significant effect on blood pressure (Table 4). Histological analysis demonstrated that both Ang II–induced cardiomyocyte hypertrophy and fibrosis were significantly attenuated when WT and HMGB1-Tg mice were treated with the ATM inhibitor after Ang II infusion compared with that of WT and HMGB1-Tg mice treated with vehicle after Ang II infusion (Figures 7C to 7E). These results suggest that pharmacological ATM inhibition preserves cardiac function and reduces cardiac hypertrophy and fibrosis after Ang II infusion.

DISCUSSION

Our study shows that nuclear HMGB1 expression was decreased and phosphorylation of ATM was increased in the failing human heart. Decreased nuclear HMGB1 expression in failing human hearts was associated with cardiomyocyte hypertrophy, fibrosis, and high serum BNP levels. Both in vivo and in vitro studies revealed that cardiac nuclear HMGB1 prevented Ang II–induced pathological cardiac hypertrophy through inhibition of the DDR pathway. Mechanistically, cardiac nuclear HMGB1 inhibited phosphorylation of ATM and subsequent activation of ERK 1/2 and NF-κB signaling. Moreover, a specific ATM inhibitor, KU55933, prevented Ang II–induced

FIGURE 5 Effect of HMGB1 Suppression on DNA Damage and DDR After Ang II Stimulation

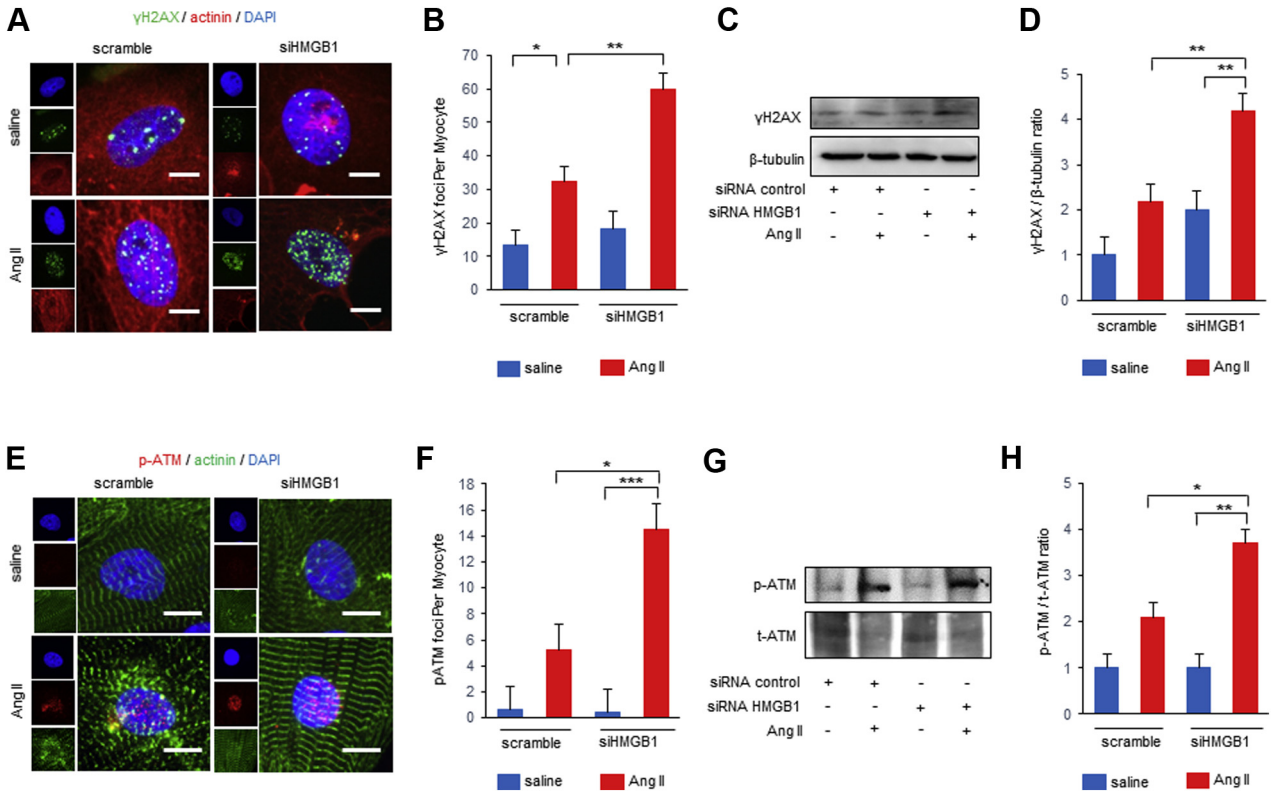

(A, B) Representative images and analysis of immunostaining of nuclear foci of γ-H2AX **(green)**, α-actinin **(red)**, and DAPI **(blue)** of NRCMs transfected with small interfering HMGB1 (siHMGB1) or nonspecific control small interfering ribonucleic acid (siRNA) and then treated with saline or Ang II for 24 h. The foci number of γ-H2AX per NRCM was counted. Scale bars = 20 μm. n = 6 in scramble saline group; n = 6 in scramble Ang II group; n = 5 in siHMGB1 saline group; n = 6 in siHMGB1 Ang II group. **(C, D)** Representative images and analysis of Western blots of γ-H2AX. NRCMs transfected with siHMGB1 or nonspecific control siRNA and then treated with saline or Ang II for 24 h (n = 6 per group). **(E, F)** Representative images and analysis of immunostaining of nuclear foci of p-ATM **(red)**, α-actinin **(green)**, and DAPI **(blue)** of NRCMs transfected with siHMGB1 or nonspecific control siRNA and then treated with saline or Ang II for 24 h. The foci number of p-ATM per NRCM was counted. Scale bars = 20 μm. n = 5 in scramble saline group; n = 4 in scramble Ang II group; n = 5 in siHMGB1 saline group; n = 4 in siHMGB1 Ang II group. **(G, H)** Representative images and analysis of Western blots of p-ATM and total ATM. NRCMs transfected with siHMGB1 or nonspecific control siRNA and then treated with saline or Ang II for 24 h (n = 3 per group). Results are presented as the mean ± SE. *p < 0.05; **p < 0.01; ***p < 0.001. Abbreviations as in Figures 1–4.

pathological cardiac remodeling. These results provide new insight into the pathogenesis of cardiac remodeling and therapeutic potential of HMGB1-DDR axis.

In the present study, we showed that cardiac nuclear HMGB1 plays a protective role in Ang II–induced cardiac hypertrophy, suggesting that cardiac nuclear HMGB1 is one of the key regulator of pathological cardiac remodeling. HMGB1 is a nonhistone nuclear protein and a member of the HMG protein superfamilies. HMGB1 is the most abundant HMG protein and has multiple functions both inside and outside of the cell. Extracellular HMGB1 acts as a DAMP, which causes various inflammatory and immune responses (28). Extracellular HMGB1 causes cardiac hypertrophy and worsens ischemia or reperfusion injury, myocardial inflammation, and fibrosis (11–13). Thus, several studies have demonstrated the role of extracellular HMGB1 in cardiac remodeling. However, the role of intracellular HMGB1, especially nuclear HMGB1, in cardiac remodeling is poorly defined. We previously reported that cardiac nuclear HMGB1 protected against pressure overload induced heart failure and doxorubicin-induced cardiomyopathy (17,25). The protective roles of nuclear HMGB1 are further supported by the findings that ablation of nuclear HMGB1 worsens acute pancreatitis, liver ischemia and reperfusion injury, and bacterial infection (14,15,29). Consistent with these studies, our results show the cardioprotective role of cardiac nuclear HMGB1 on pathological cardiac hypertrophy and fibrosis.

FIGURE 6 Effect of HMGB1 and ATM on Cardiac Hypertrophic Signaling

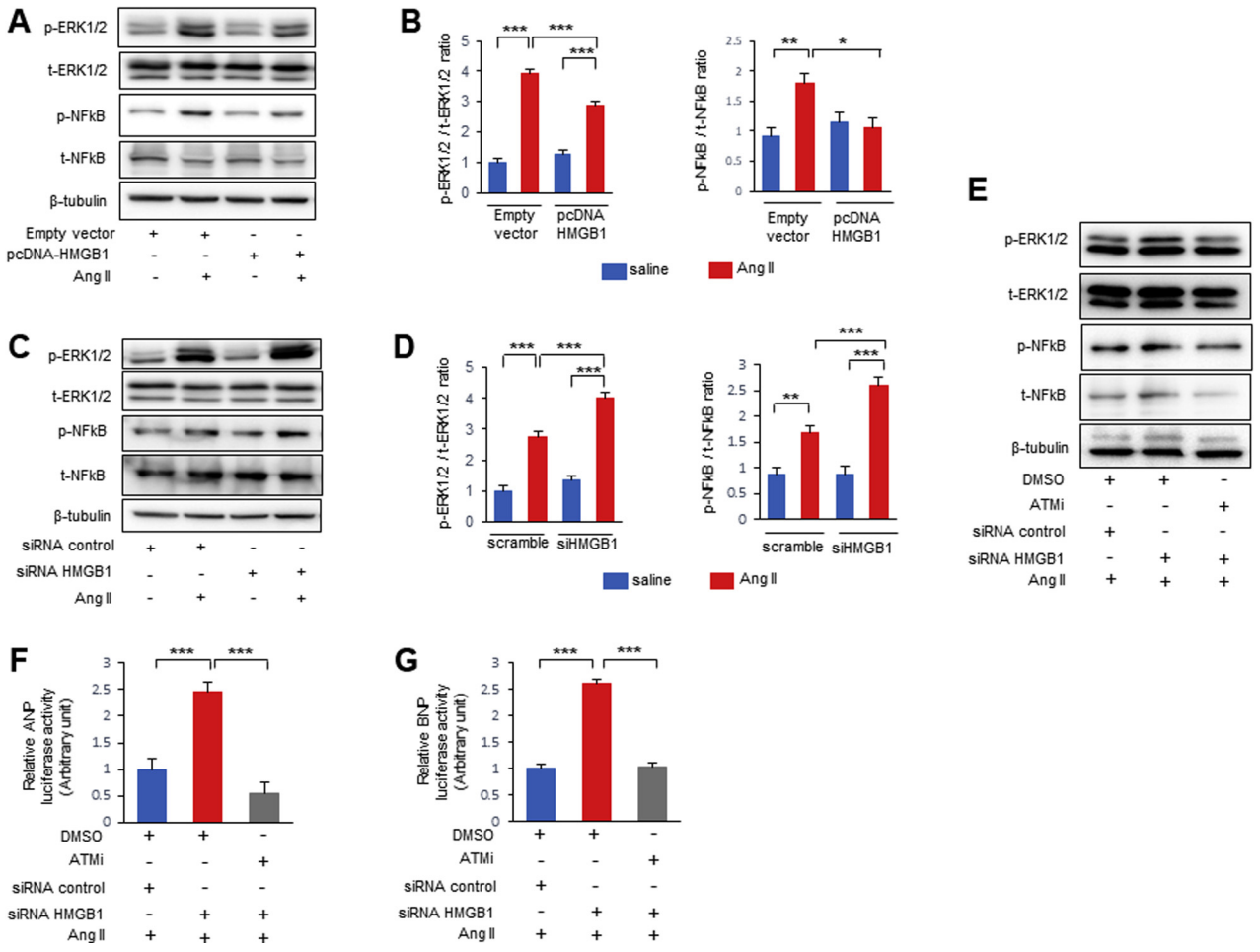

(A, B) Representative images and analysis Western blots of phospho-extracellular signal-related kinase 1/2 (p-ERK1/2), total ERK1/2 (t-ERK1/2), phospho-nuclear factor kappa B (p-NF-κB), and total NF-κB (t-NF-κB) from NRCMs transfected with pcDNA-HMGB1 or control vector and then treated with saline or Ang II for 4 h (n = 6 per group). **(C, D)** Representative images and analysis of Western blots of p-ERK1/2, t-ERK1/2, p-NF-κB, and t-NF-κB from NRCMs transfected with siHMGB1 or nonspecific control siRNA and then treated with saline or Ang II for 4 h (n = 6 per group). **(E)** Representative Western blots of p-ERK1/2, t-ERK1/2, p-NF-κB, and t-NF-κB. NRCMs transfected with siHMGB1 or nonspecific control siRNA were pretreated with an ATM inhibitor (KU55933) or dimethyl sulfoxide (DMSO) for 1 h before Ang II stimulation, and then stimulated with saline or Ang II for 4 h. **(F, G)** Quantification of atrial natriuretic peptide (ANP) and BNP promoter activities. Rat H9C2 cells were pretreated with an ATM inhibitor (KU55933) or DMSO for 1 h before Ang II stimulation, and then stimulated with saline or Ang II for 24 h (n = 6 per group). Results are presented as the mean ± SE. *p < 0.05; **p < 0.01; ***p < 0.001. Abbreviations as in Figures 1 to 5.

The present study showed that cardiac nuclear HMGB1 prevented cardiomyocytes against DNA damage and following DDR activation because HMGB1 prevented upregulation of γ-H2AX, a specific marker of DNA damage, and p-ATM. Intracellular HMGB1 has various functions such as DNA chaperone, DNA repair, chromosome guardian, autophagy sustainer, and protector from apoptotic cell death. Loss of nuclear HMGB1 caused decreased chromatin accessibility to repair DNA damage, resulted in nuclear catastrophe, and subsequent cell death (14,15). These studies indicate the role of nuclear HMGB1 as a defender against cellular DNA damage in several disease conditions. In the heart, significantly more DNA damage was observed in heart failure patients compared with that of normal-health control subjects (19). In the experimental model, DNA damage was also observed in a mouse model of myocardial infarction, which was associated with cell apoptosis (30). Excessive DNA damage causes phosphorylation of ATM, a key regulator of DDR, and contributes to several disease conditions, including heart failure.

FIGURE 7 Cardioprotective Effect of the ATM Inhibitor on Ang II-Induced Pathological Cardiac Remodeling

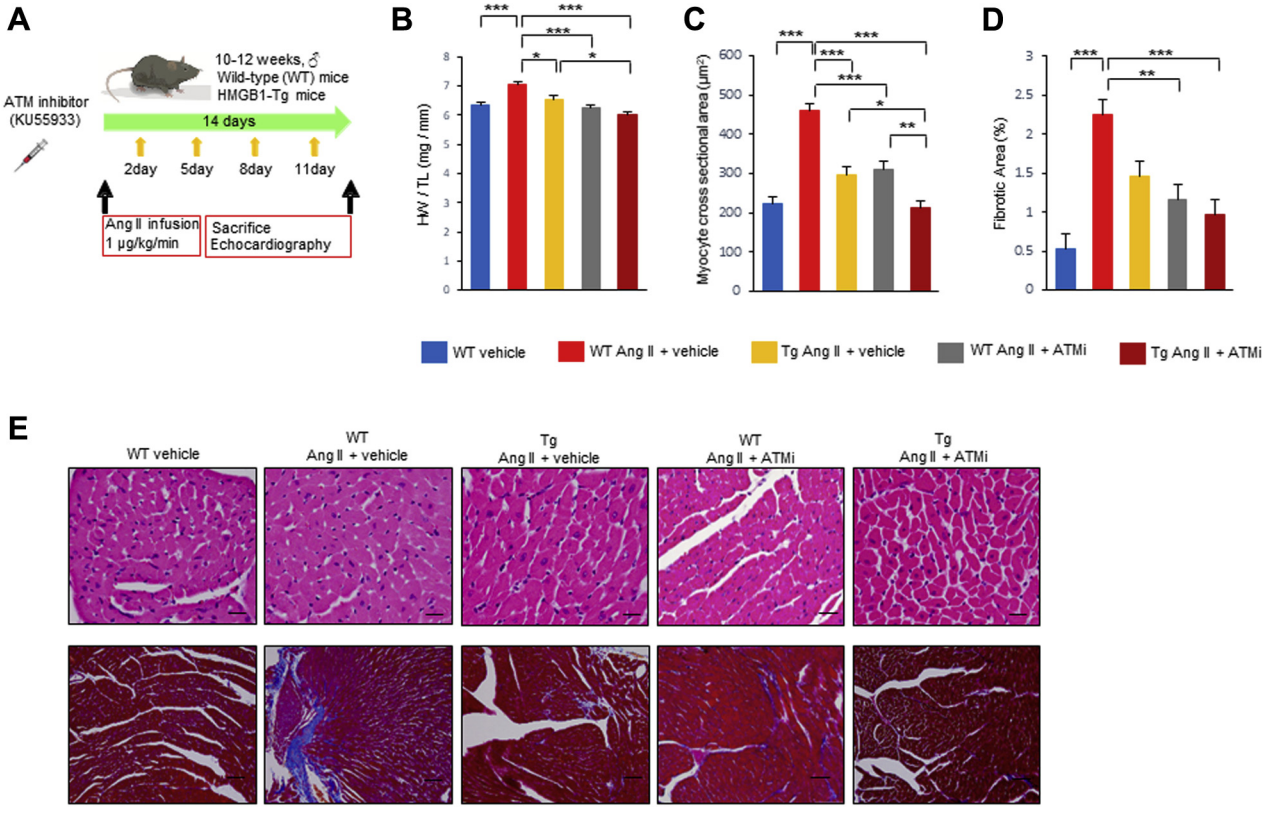

(A) Timeline of Ang II infusion and ATM inhibitor (KU55933) or vehicle administration in mice. **(B)** The ratio of HW/TL in WT and HMGB1-Tg mice subjected to Ang II infusion and vehicle or ATM inhibitor (KU55933) treatment (n = 8 in WT vehicle group; n = 8 in WT Ang II + vehicle group; n = 6 in HMGB1-Tg Ang II + vehicle group; n = 6 in WT Ang II + KU55933 group; n = 6 in HMGB1-Tg Ang II + KU55933 group). **(C)** Analysis of CM cross-sectional area by H&E staining in left ventricular sections in WT and HMGB1-Tg mice subjected to Ang II infusion and vehicle or ATM inhibitor (KU55933) treatment (n = 10 in WT vehicle group; n = 10 in WT Ang II + vehicle group; n = 9 in HMGB1-Tg Ang II + vehicle group; n = 7 in WT Ang II + KU55933 group; n = 9 in HMGB1-Tg Ang II + KU55933 group). **(D)** Analysis of cardiac fibrosis by Masson's trichrome staining in left ventricular sections in WT and HMGB1-Tg mice subjected to Ang II infusion and vehicle or ATM inhibitor (KU55933) treatment (n = 6 per group). **(E)** Representative images of CM cross-sectional area by H&E staining (Scale bars = 20 μm) and cardiac fibrosis by Masson's trichrome staining (Scale bars = 50 μm) in left ventricular sections in WT and HMGB1-Tg mice subjected to Ang II infusion and vehicle or ATM inhibitor (KU55933) treatment. Results are presented as the mean ± SE. *p < 0.05; **p < 0.01; ***p < 0.001. Abbreviations as in Figures 1 to 6.

TABLE 3 Echocardiographic Data of WT and HMGB1-Tg Mice Subjected to Ang II Infusion and Vehicle or ATMi Treatment

	WT Vehicle (n = 9)	WT Ang II + Vehicle (n = 10)	HMGB1-Tg Ang II + Vehicle (n = 6)	WT Ang II + ATMi (n = 6)	HMGB1-Tg Ang II + ATMi (n = 6)
LVDd, mm	3.15 ± 0.15	3.04 ± 0.14	3.36 ± 0.18	2.96 ± 0.18	3.32 ± 0.18
LVDs, mm	1.63 ± 0.11	1.76 ± 0.10	1.89 ± 0.13	1.40 ± 0.13	1.72 ± 0.13
IVSd, mm	0.74 ± 0.03	1.04 ± 0.03*	0.85 ± 0.04†	0.80 ± 0.04‡	0.70 ± 0.05‡
PWd, mm	0.76 ± 0.03	1.00 ± 0.03*	0.88 ± 0.04	0.80 ± 0.04†	0.75 ± 0.04‡
FS, %	48.6 ± 1.6	42.5 ± 1.5	43.2 ± 2.0	52.3 ± 2.0†	48.6 ± 2.0
E/A ratio	1.84 ± 0.06	1.13 ± 0.06*	1.41 ± 0.07§	1.68 ± 0.07‡	2.02 ± 0.07‡

Values are mean ± SE. *p < 0.001 versus WT vehicle mice. †p < 0.01versus WT Ang II mice. ‡p < 0.001 versus WT Ang II mice. §p < 0.05versus WT Ang II mice.
ATMi = ataxia telangiectasia mutated inhibitor; other abbreviations as in Table 1.

Phosphorylation of ATM was increased in end-stage failing human hearts, and prolonged mechanical unload by left ventricular assist device implantation decreased the expression of p-ATM in cardiomyocytes, which was associated with a reduction of cardiomyocyte cell size (31). In addition, a recent study demonstrated that DNA damage-induced ATM activation caused pressure overload induced heart failure in mice. Activation of ATM caused increases in inflammatory cytokines thorough NF-κB signaling. Those effects were rescued by ATM deletion, and the ATM deletion prevented heart failure progression in mice, suggesting a causative role for ATM in heart failure (32). These studies support the crucial role of

ATM in cardiac hypertrophy. Our study also demonstrated that HMGB1 interacts with ATM, and Ang II stimulation weakened the interaction and subsequent ATM activation. These results suggest that ATM activation was mediated, at least in part, by HMGB1. Thus, ATM is one of the important target molecules of HMGB1 in pathological cardiac hypertrophy.

ATM has crucial roles in the development of pathological cardiac remodeling. However, it remains unclear whether pharmacological ATM inhibition protects against pathological cardiac remodeling. In the present study, we demonstrated for the first time that ATM inhibitor treatment offered a synergic cardioprotective effect in WT and HMGB1-Tg mice against Ang II–induced cardiac hypertrophy and fibrosis. In addition, ATM inhibitor treatment suppressed Ang II–induced ANP and BNP activation and phosphorylation of ERK1/2 and NF-κB in vitro. KU55933 is a potent and selective inhibitor of ATM and is developed as an anticancer therapy (33). In addition to being an anticancer therapy, KU55933 provided protective effect against oxidative damage, inflammation, and senescence (34,35). Furthermore, KU55933 attenuated doxorubicin-induced cardiac dysfunction (36). Several studies demonstrated that ERK1/2 is involved in pathological cardiomyocyte hypertrophy (37,38). DNA damage causes ATM dependent NF-κB activation, and NF-κB activation is reported to be associated with pathological cardiac remodeling (39,40). Our results indicate that ATM inhibition prevented Ang II–induced pathological cardiac remodeling by targeting ERK1/2 and NF-κB pathways. In the present study, KU55933 provides the synergistic cardioprotective effect for Ang II–induced pathological cardiac remodeling in HMGB1-Tg mice. This cardioprotective effect of KU55933 in HMGB1-Tg mice might be contributed to that DNA damage was also mediated by other mechanisms in addition to nuclear HMGB1 (30,41–44). The present study demonstrated for the first time, the involvement of the HMGB1-ATM axis in pathological cardiac remodeling, and provided potential therapeutic efficacy of targeting DDR inhibition.

STUDY LIMITATIONS. First, we did not evaluate the effect of loss of cardiac nuclear HMGB1 on pathological cardiac remodeling in vivo, although we evaluated those effect in vitro using siHMGB1. A previous study showed that specific deletion of HMGB1 in cardiomyocytes did not affect cardiac function at baseline (45). However, the effect of cardiomyocyte specific HMGB1 deletion under stress conditions is still unclear. Second, our study could not rule out the possible protective effect of ATM inhibitor KU55933 on other cell types in vivo, although we confirmed the cardiomyocyte-specific protective effect of KU55933 in vitro. A previous study revealed that fibroblast-specific ATM knockout mice attenuated doxorubicin-induced cardiotoxicity (36). Third, we have not evaluated the effect of extracellular HMGB1 in both in vivo and in vitro studies. Because extracellular HMGB1 acts as DAMPs and affects reparative immune responses (9,10), extracellular HMGB1 may influence Ang II–induced pathological cardiac remodeling.

TABLE 4 Hemodynamic Data of WT and HMGB1-Tg Mice Subjected to Ang II Infusion and Vehicle or ATMi Treatment

	WT Vehicle (n = 15)	WT Ang II + Vehicle (n = 12)	HMGB1-Tg Ang II + Vehicle (n = 11)	WT Ang II + ATMi (n = 14)	HMGB1-Tg Ang II + ATMi (n = 9)
BW, g	26.4 ± 0.7	26.9 ± 0.7	25.9 ± 0.9	25.9 ± 0.7	24.8 ± 0.9
Hemodynamic parameter					
HR, beats/min	601 ± 20	582 ± 23	600 ± 24	619 ± 21	573 ± 26
SBP, mm Hg	93 ± 5	138 ± 6*	141 ± 6*	138 ± 5*	147 ± 6*
DBP, mm Hg	39 ± 7	87 ± 8*	71 ± 8†	71 ± 7‡	81 ± 9‡
MBP, mm Hg	57 ± 6	104 ± 7*	94 ± 7‡	93 ± 6‡	99 ± 8‡

Values are mean ± SE. *$p < 0.001$ versus WT vehicle mice. †$p < 0.05$ versus WT vehicle mice. ‡$p < 0.01$ versus WT vehicle mice.

Abbreviations as in Tables 1 to 3.

CONCLUSIONS

Our study documents a novel mechanism by which cardiac nuclear HMGB1 attenuates Ang II–induced pathological cardiac remodeling through inhibition of ATM activation. Furthermore, targeting DDR treatment by using a novel selective ATM inhibitor KU55933 prevents Ang II–induced pathological cardiac remodeling. This work provides further evidence of critical role of cardiac nuclear HMGB1 in the development of pathological cardiac remodeling, and possibly the development of novel therapeutics for heart failure treatment.

ACKNOWLEDGMENTS The authors thank Ms. Emiko Nishidate and Ms. Yuko Sasaki for their excellent technical assistance and comments. The authors thank Editage for the English language review.

ADDRESS FOR CORRESPONDENCE: Dr. Tetsuro Shishido, Department of Cardiology, Pulmonology, and Nephrology, Yamagata University School of Medicine, 2-2-2 Iida-nishi, Yamagata 990-9585, Japan. E-mail: tshishid@med.id.yamagata-u.ac.jp.

PERSPECTIVES

COMPETENCY IN MEDICAL KNOWLEDGE: Cardiac nuclear-specific HMGB1 overexpression in cardiomyocytes reduces left ventricular hypertrophy and remodeling after Ang II stimulation. Cardiac nuclear HMGB1 prevents cardiomyocyte DDR, which is associated with developing heart failure.

TRANSLATIONAL OUTLOOK: Further research is needed to explore the therapeutic potential of nuclear HMGB1 and DDR axis for patients with heart failure.

REFERENCES

1. Mozaffarian D, Benjamin EJ, Go AS, et al. Heart disease and stroke statistics–2015 update: a report from the American Heart Association. Circulation 2015;131:e29–322.

2. Ambrosy AP, Fonarow GC, Butler J, et al. The global health and economic burden of hospitalizations for heart failure: lessons learned from hospitalized heart failure registries. J Am Coll Cardiol 2014;63:1123–33.

3. Val-Blasco A, Piedras MJ, Ruiz-Hurtado G, et al. Role of NOD1 in heart failure progression via regulation of Ca2+ handling. J Am Coll Cardiol 2017;69:423–33.

4. Jessup M, Brozena S. Heart failure. N Engl J Med 2003;348:2007–18.

5. McMurray JJ, Pfeffer MA. Heart failure. Lancet 2005;365:1877–89.

6. Braunwald E. The war against heart failure: the Lancet lecture. Lancet 2015;385:812–24.

7. Nightingale K, Dimitrov S, Reeves R, Wolffe AP. Evidence for a shared structural role for HMG1 and linker histones B4 and H1 in organizing chromatin. EMBO J 1996;15:548–61.

8. Lange SS, Mitchell DL, Vasquez KM. High mobility group protein B1 enhances DNA repair and chromatin modification after DNA damage. Proc Natl Acad Sci U S A 2008;105:10320–5.

9. Lotze MT, Tracey KJ. High-mobility group box 1 protein (HMGB1): nuclear weapon in the immune arsenal. Nat Rev Immunol 2005;5:331–42.

10. Turner NA. Inflammatory and fibrotic responses of cardiac fibroblasts to myocardial damage associated molecular patterns (DAMPs). J Mol Cell Cardiol 2016;94:189–200.

11. Su FF, Shi MQ, Guo WG, et al. High-mobility group box 1 induces calcineurin-mediated cell hypertrophy in neonatal rat ventricular myocytes. Mediators Inflamm 2012;2012:805149.

12. Andrassy M, Volz HC, Igwe JC, et al. High-mobility group box-1 in ischemia-reperfusion injury of the heart. Circulation 2008;117:3216–26.

13. Zhang W, Lavine KJ, Epelman S, et al. Necrotic myocardial cells release damage-associated molecular patterns that provoke fibroblast activation in vitro and trigger myocardial inflammation and fibrosis in vivo. J Am Heart Assoc 2015;4:e001993.

14. Kang R, Zhang Q, Hou W, et al. Intracellular Hmgb1 inhibits inflammatory nucleosome release and limits acute pancreatitis in mice. Gastroenterology 2014;146:1097–107.

15. Huang H, Nace GW, McDonald KA, et al. Hepatocyte-specific high-mobility group box 1 deletion worsens the injury in liver ischemia/reperfusion: a role for intracellular high-mobility group box 1 in cellular protection. Hepatology 2014;59:1984–97.

16. Messer J, Chang E. Intracellular HMGB1: defender of client proteins and cell fate. Oncotarget 2015;6:8432–3.

17. Funayama A, Shishido T, Netsu S, et al. Cardiac nuclear high mobility group box 1 prevents the development of cardiac hypertrophy and heart failure. Cardiovasc Res 2013;99:657–64.

18. Sulli G, Di Micco R, d'Adda di Fagagna F. Crosstalk between chromatin state and DNA damage response in cellular senescence and cancer. Nat Rev Cancer 2012;12:709–20.

19. Siggens L, Figg N, Bennett M, Foo R. Nutrient deprivation regulates DNA damage repair in cardiomyocytes via loss of the base-excision repair enzyme OGG1. FASEB J 2012;26:2117–24.

20. Shukla PC, Singh KK, Quan A, et al. BRCA1 is an essential regulator of heart function and survival following myocardial infarction. Nat Commun 2011;2:593.

21. Sano M, Minamino T, Toko H, et al. p53-induced inhibition of Hif-1 causes cardiac dysfunction during pressure overload. Nature 2007;446:444–8.

22. Aoki T, Fukumoto Y, Sugimura K, et al. Prognostic impact of myocardial interstitial fibrosis in non-ischemic heart failure. Comparison between preserved and reduced ejection fraction heart failure. Circ J 2011;75:2605–13.

23. Lorenzen JM, Schauerte C, Hubner A, et al. Osteopontin is indispensible for AP1-mediated angiotensin II-related miR-21 transcription during cardiac fibrosis. Eur Heart J 2015;36:2184–96.

24. Shishido T, Nozaki N, Yamaguchi S, et al. Toll-like receptor-2 modulates ventricular remodeling after myocardial infarction. Circulation 2003;108:2905–10.

25. Narumi T, Shishido T, Otaki Y, et al. High-mobility group box 1-mediated heat shock protein beta 1 expression attenuates mitochondrial dysfunction and apoptosis. J Mol Cell Cardiol 2015;82:1–12.

26. Honda Y, Shishido T, Takahashi T, et al. Midkine deteriorates cardiac remodeling via epidermal growth factor receptor signaling in chronic kidney disease. Hypertension 2016;67:857–65.

27. Bonner WM, Redon CE, Dickey JS, et al. GammaH2AX and cancer. Nat Rev Cancer 2008;8:957–67.

28. Kang R, Chen R, Zhang Q, et al. HMGB1 in health and disease. Mol Aspects Med 2014;40:1–116.

29. Yanai H, Matsuda A, An J, et al. Conditional ablation of HMGB1 in mice reveals its protective function against endotoxemia and bacterial infection. Proc Natl Acad Sci U S A 2013;110:20699–704.

30. Wo D, Peng J, Ren DN, et al. Opposing roles of Wnt inhibitors IGFBP-4 and Dkk1 in cardiac ischemia by differential targeting of LRP5/6 and beta-catenin. Circulation 2016;134:1991–2007.

31. Canseco DC, Kimura W, Garg S, et al. Human ventricular unloading induces cardiomyocyte proliferation. J Am Coll Cardiol 2015;65:892–900.

32. Higo T, Naito AT, Sumida T, et al. DNA single-strand break-induced DNA damage response causes heart failure. Nat Commun 2017;8:15104.

33. Zhang T, Shen Y, Chen Y, Hsieh JT, Kong Z. The ATM inhibitor KU55933 sensitizes radioresistant bladder cancer cells with DAB2IP gene defect. Int J Rad Biol 2015;91:368–78.

34. Chwastek J, Jantas D, Lason W. The ATM kinase inhibitor KU-55933 provides neuroprotection against hydrogen peroxide-induced cell damage via a gammaH2AX/p-p53/caspase-3-independent mechanism: Inhibition of calpain and cathepsin D. Int J Biochem Cell Biol 2017;87:38–53.

35. Kang C, Xu Q, Martin TD, et al. The DNA damage response induces inflammation and senescence by inhibiting autophagy of GATA4. Science 2015;349:aaa5612.

36. Zhan H, Aizawa K, Sun J, et al. Ataxia telangiectasia mutated in cardiac fibroblasts regulates doxorubicin-induced cardiotoxicity. Cardiovasc Res 2016;110:85–95.

37. Yu CJ, Tang LL, Liang C, et al. Angiotensin-converting enzyme 3 (ACE3) protects against pressure overload-induced cardiac hypertrophy. J Am Heart Assoc 2016;5:e002680.

38. Bueno OF, Molkentin JD. Involvement of extracellular signal-regulated kinases 1/2 in cardiac hypertrophy and cell death. Circ Res 2002;91:776–81.

39. Barroso-Gonzalez J, Auclair S, Luan S, et al. PACS-2 mediates the ATM and NF-kappaB-dependent induction of anti-apoptotic Bcl-xL in response to DNA damage. Cell Death Differ 2016;23:1448–57.

40. Zhao QD, Viswanadhapalli S, Williams P, et al. NADPH oxidase 4 induces cardiac fibrosis and hypertrophy through activating Akt/mTOR and NFkappaB signaling pathways. Circulation 2015;131:643–55.

41. Gray K, Kumar S, Figg N, et al. Effects of DNA damage in smooth muscle cells in atherosclerosis. Circ Res 2015;116:816–26.

42. Zhou J, Ahmad F, Parikh S, et al. Loss of adult cardiac myocyte GSK-3 leads to mitotic catastrophe resulting in fatal dilated cardiomyopathy. Circ Res 2016;118:1208–22.

43. Tumurkhuu G, Shimada K, Dagvadorj J, et al. Ogg1-dependent DNA repair regulates NLRP3 inflammasome and prevents atherosclerosis. Circ Res 2016;119:e76–90.

44. Boon RA, Iekushi K, Lechner S, et al. MicroRNA-34a regulates cardiac ageing and function. Nature 2013;495:107–10.

45. Huebener P, Gwak GY, Pradere JP, et al. High-mobility group box 1 is dispensable for autophagy, mitochondrial quality control, and organ function in vivo. Cell Metab 2014;19:539–47.

KEY WORDS DNA damage response, HMGB1, pathological cardiac hypertrophy

APPENDIX For expanded Methods and References sections, please see the online version of this article.